

## Modeling of Anaerobic Digestion of Complex Substrates

**Keshtkar, Ali Reza**

Atomic Energy Organization of Iran, P.O. Box 11365-8486, Tehran, I.R. IRAN &  
Department of Chemical Engineering, Tehran University, P.O. Box 11365-4563, Tehran, I.R. IRAN

**Abolhamd, Gity\*<sup>+</sup>**

Department of Chemical Engineering, Tehran University, P.O. Box 11365-4563, Tehran, I.R. IRAN

**Meyssami, Behrooz**

Department of Chemical Engineering, Tehran University, P.O. Box 11365-4563, Tehran, I.R. IRAN

**Ghaforian, Hossein**

Atomic Energy Organization of Iran, P.O. Box 11365-8486, Tehran, I.R. IRAN

**ABSTRACT:** A structured mathematical model of anaerobic conversion of complex organic materials in non-ideally cyclic-batch reactors for biogas production has been developed. The model is based on multiple-reaction stoichiometry (enzymatic hydrolysis, acidogenesis, acetogenesis and methanogenesis), microbial growth kinetics, conventional material balances in the liquid and gas phases for a cyclic-batch reactor, liquid-gas interactions, liquid-phase equilibrium reactions and a simple mixing model which considers the reactor volume in two separate sections: the flow-through and the retention regions. The dynamic model describes the effects of reactant distribution resulting from the mixing conditions, time interval of feeding, hydraulic retention time and mixing parameters on the process performance. The model is applied in the simulation of anaerobic digestion of cattle manure under different operating conditions. The model is compared with experimental data and good correlations are obtained.

**KEY WORDS:** Anaerobic digestion, Dynamic modeling, Two-region mixing model, Cyclic-batch reactor, Complex substrates, Biogas

### INTRODUCTION

In the past 30 years a number of different anaerobic processes have been developed. Modeling studies are

important because the experiments on the process are very time-consuming, labor intensive

---

\* To whom correspondence should be addressed.

+ E-mail : [abolhamd@ut.ac.ir](mailto:abolhamd@ut.ac.ir)

1021-9986/03/2/61

12/\$/3.20

expensive. The development of an up-to-date model for anaerobic digestion of organic matter is accomplished with considerable difficulties, due to the numerous variables existing in the anaerobic system. Large-scale anaerobic digestion of organic wastes has received growing attention during the recent years in Iran and elsewhere as a more efficient method for utilizing organic wastes for the production of energy and fertilizer [1]. Consequently, the need for accurate modeling of the anaerobic degradation of complex wastes has increased in recent years. The simplified models such as those by Andrews [2] and Buhr [3] have only considered the acetic degradation rate. Hill and Barth [4] included the hydrolysis and the acidogenesis steps in computing the organic overload effect in the methane production rate. Angelidaki [5] developed a structured kinetic model for ideal CSTR reactors. Today there are reports of rigorous simulators that consider the different phenomena involved, such as inhibition, ionic equilibrium, gas-liquid transfer and biofilm growth [6,7,8,9].

In general, all these models describe the ideal bioreactors but not the real systems. In real systems, the mixing device is an important component of the reactor. Good mixing promotes the effective transfer of the substrates and heat to the microorganisms, maintains uniformity in the other environmental factors and assures the effective use of the entire reactor volume by preventing stratification. Conversely, incomplete mixing jeopardizes the efficiency of the treatment process and therefore, the stability of the sludge produced. Scum formation can also be greatly reduced or even eliminated by suitable agitation. It is recognized that heterogeneities in the medium can have a profound influence, especially, on the production of the metabolites [10].

While the imperfect mixing patterns are more common than the ideal ones in a real reactor, the anaerobic digestion models often assume the complete mixing conditions. The ideal assumption of the completely mixed reactors may be valid in some cases, where due to the small scale of the experimental reactors used, perfect mixing may effectively be achieved or when the characteristic time constants for the kinetic parameters are much larger than the mixing and the mass transfer time constants. However, the difficulty in achieving complete mixing increases with the reactor size

and as a result, the inevitable compromises increasing costs and the loss of the equipment mixing in the large reactors may not be as good as the small ones. The residence time distribution conducted in the full-scale primary digesters showed that the actively mixed volumes can be as low as 10% of the total volume [11].

Farm animals are ideal for the application of anaerobic digestion to convert cattle manure to energy generation and fertilizer product. Cattle manure is a complex substrate containing organic and the insoluble organic matter such as polysaccharides, lipids, proteins, and the volatile fatty acids. A cyclic batch operation is one of the most common methods for the animal waste treatment. Most of the previous researches on the dairy wastewater treatment have been based on this type of the anaerobic digestion [5,12,13,14].

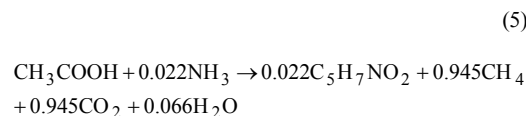
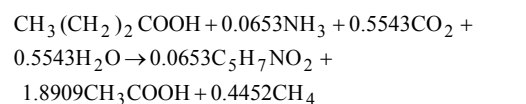
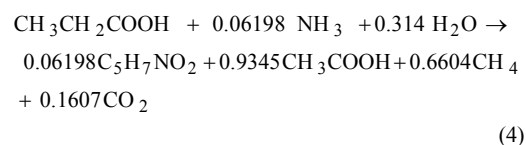
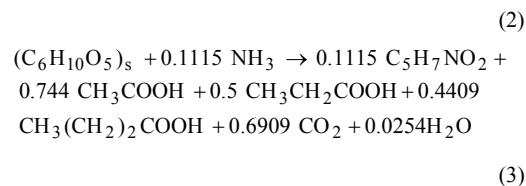
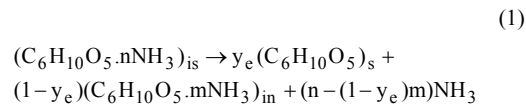
The objective of this paper is to present a kinetic model for the anaerobic digestion of complex substrates such as cattle manure in a cyclic batch reactor. The model satisfies the following criteria:

- 1- Making a model capable of considering all the important factors involved in the anaerobic process.
- 2- Reducing the dimensions of the model so that the needed numerical calculations could be carried out on a personal computer.
- 3- Providing a rational explanation of the effects between mixing parameters and digestion kinetics in non-ideal cyclic batch reactors.

#### Microbial kinetic model

The kinetic model used in this study is based on the Angelidaki [16] kinetic model for the anaerobic digestion of the cattle manure. The kinetic model distinguishes different processes: the hydrolysis of the complex substrate by the extracellular enzymes, the consumption of the soluble substrates by the acidogenic bacteria, the consumption of the volatile fatty acids (VFAs) by the acetogenic bacteria, the formation of acetate by the propionate-degrading acetogenic bacteria, and the consumption of acetate and the generation of methane by the methanogenic bacteria. The model includes the inhibition of the hydrolysis step, the acetate inhibition in the acetogenic steps, the free ammonia inhibition in the methanogenic step and the pH inhibition

biological steps. In the model the primary substrates in the manure are represented as the soluble (s) and the insoluble (is) carbohydrate units, with the basic formula  $(C_6H_{10}O_5)_s$  and  $(C_6H_{10}O_5.nNH_3)_{is}$  respectively. The cell mass is represented by the empirical formula  $C_5H_7O_2N$ . Also it is assumed that the volatile fatty acids contain only the acetic, the propionic and the butyric acids. The model expressions are as follow:



In Reaction 1,  $y_e$  is the enzymatic efficiency or yield factor and the subscript *in* represents the undegradable inert organic material. The coefficients  $y_e$ ,  $n$ , and  $m$ , together with the ratio of the soluble to the insoluble substrate depend on the type of the manure. In the model, the hydrolytic step and the biomass decay are described by the first order kinetics, while the consumption of the soluble substrates and the volatile acids as well as the growth of the anaerobic microorganisms are assumed to obey the Monod-type kinetics with the noncompetitive inhibition function of the intermediate substrates and the pH inhibition on the microbial growth rates, according to the expressions presented in the following:

The hydrolysis rate:

$$r_h = k C_{is}$$

$$k = k_0 \frac{k_{i,VFA}}{\sum VFA + k_{i,VFA}}$$

$$\sum VFA = C_{ac} + f_{pr} C_{pr} + f_{but} C_{but}$$

The biomass decay rate, the substrate consumption rate and the biomass growth rate respectively as follow:

$$r_d = k_d X$$

$$r_s = Y_{s/x} \mu X$$

$$r_x = \mu X$$

The specific growth rates are as follow:

$$\mu_A = \mu_{maxA} \frac{C_s}{K_{ss} + C_s}$$

$$\mu_{AP} = \mu_{maxAP} \frac{C_{pr}}{K_{spr} + C_{pr}} \times \frac{K_{ipr}}{K_{ipr} + C_{ac}} \times F_{AP}(pH)$$

$$\mu_{AB} = \mu_{maxAB} \frac{C_{but}}{K_{sbut} + C_{but}} \times \frac{K_{ibut}}{K_{ibut} + C_{ac}} \times F_{AB}(pH)$$

$$\mu_M = \mu_{maxM} \frac{C_{ac}}{K_{sac} + C_{ac}} \times \frac{K_{iam}}{K_{iam} + C_{am}} \times F_M(pH)$$

$$F(pH) = \frac{1 + 2 \times 10^{0.5(pK_1 - pH)}}{1 + 10^{(pH - pK_h)} + 10^{(pK_1 - pH)}}$$

#### Liquid mixing model

A simple mixing model referred to as the model was used in combination with the kinetic conceptual representation of the two-region model is illustrated in Figure 1. The model assumes that the reactor volume is split into the flow-through ( $\alpha$ ) region and the retention. Both regions are assumed to be perfectly mixed. The transfer of the materials between the zones is bidirectional. The flow-through region has the features of the behavior of the retention region.

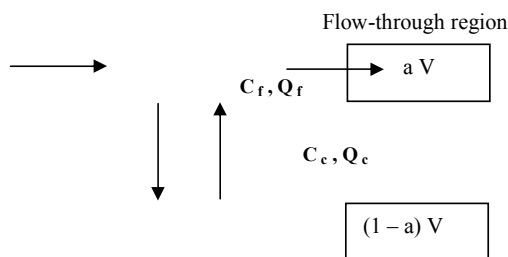


Fig. 1: Two-region mixing model

a stagnant zone. The different levels of mixing are accomplished by adjusting the relative volume of the flow-through region ( $a$ ) and the ratio of the exchange flow rate between regions to the feed flow rate ( $b$ ).

Despite its simplicity, this classical model is used in chemical engineering for the description of the retention time distribution in the real reactors [15] and has proved to be a useful tool for the theoretical study of the effects of heterogeneity in the chemical and biological systems. By definition, for a relative volume in the flow-through region ( $a$ ) close to unity and, for any value of ' $a$ ', with an interchange rate of the material between regions to the feed flow rate ratio ( $b$ ) approaching infinity, the dynamic model produces results closely approaching those of a completely mixed reactor. Otherwise, for any ' $a$ ' with ' $b$ ' close to zero (i.e. no interchange of material between regions) the system consists of a reactor with a completely dead zone of volume  $(1-a)V_1$ . For values of the mixing parameters other than those mentioned above, the mathematical model simulates the performance of an imperfectly mixed digester.

#### Cyclic batch reactor

In an ideal cyclic batch reactor, a volume of the manure is rapidly introduced into the reactor. The mixture is stirred and the reaction takes place for a specified period of time. Afterwards, a volume of the reactor contents, equal to that introduced, is discharged from the reactor. The reactant medium is mixed with a new addition of feed in the following cycle with the same reaction time as in the previous one. After several cycles, and when the reactant concentrations are the same for all the input volumes fed, and the operating conditions are kept constant, the concentration of the products in the discharged volume can reach constant values. Under these conditions, the system is at quasi-steady state.

The descriptions that follow represent cycle of the batch operation, in four steps. In the first step the reactor is operated batch-wise for a time  $t_r$  known initial conditions. In this step the mass balances in the liquid phases of  $\alpha$  and  $\beta$  for volume cyclic batch reactor have been described in the next section. In the second step, after a reaction time  $t_r$ , a volume  $V_r$  of the reaction mixture is drained from the reactor. In the third step the reactor is filled to its original volume with the feed. Finally the reaction mixture is mixed in the last step and the initial conditions for the new cycle are obtained.

The characteristic parameters of the cyclic batch reactor are the interval of feeding time ( $t_f$ ) and the remaining volume in the reactor to be discharged from the reactor ( $R$ ):

$$t_r = \frac{V_r}{Q_f}$$

$$R = \frac{a V_1 - V_r}{V_r}$$

Therefore, the initial conditions for any new cycle are described by the relation:

$$C_i = \frac{C_f + R C_r}{R + 1}$$

Also the relation between the interval of feeding time and the hydraulic retention time (HRT) is as follows:

$$HRT = \frac{V_1}{Q_f} = \frac{t_r (R + 1)}{a}$$

The value of  $t_r$  can thus be chosen from the range  $(0, HRT)$ , hence  $R \in (0, \infty)$  respectively. If  $R \rightarrow \infty$  corresponds to the continuous flow operation and  $R=0$  denotes repeated the batch-wise operation.

#### Mathematical model

The mass balances on the  $\alpha$  and  $\beta$  liquid and gas phases of the cyclic batch reactor under different conditions for different components in the reactor led to a set of ordinary differential equations which must be simultaneously solved by the Runge-Kutta conditions. These components include the substrate, the soluble substrate, acetate, butyrate, ammonia, carbon dioxide, methanogenic bacteria, the propionate degrading

bacteria, the butyrate degrading acetogenic bacteria, and the methanogenic bacteria. The component material balances in different phases led to 25 ordinary first order differential equations and three algebraic equations as described in the following (Equations 21-38 and 41- 43).

#### Liquid phase

Biomass balance for different groups of bacteria ( $X_i$ ,  $i=A$ , AP, AB, M)

$$\frac{dX_i^\alpha}{dt} = \frac{X_i^\beta - X_i^\alpha}{a\theta/b} + (\mu_i^\alpha - b_i)X_i^\alpha \quad (21)$$

$$\frac{dX_i^\beta}{dt} = \frac{X_i^\alpha - X_i^\beta}{(1-a)\theta/b} + (\mu_i^\beta - b_i)X_i^\beta \quad (22)$$

Insoluble substrate material balance

$$\frac{dC_{is}^\alpha}{dt} = \frac{C_{is}^\beta - C_{is}^\alpha}{a\theta/b} - k^\alpha C_{is}^\alpha \quad (23)$$

$$\frac{dC_{is}^\beta}{dt} = \frac{C_{is}^\alpha - C_{is}^\beta}{(1-a)\theta/b} - k^\beta C_{is}^\beta \quad (24)$$

Soluble substrate material balance

$$\frac{dC_s^\alpha}{dt} = \frac{C_s^\beta - C_s^\alpha}{a\theta/b} + \frac{162 y_e}{162+17n} k^\alpha C_{is}^\alpha - 12.858 \mu_A^\alpha X_A^\alpha \quad (25)$$

$$\frac{dC_s^\beta}{dt} = \frac{C_s^\alpha - C_s^\beta}{(1-a)\theta/b} + \frac{162 y_e}{162+17n} k^\beta C_{is}^\beta - 12.858 \mu_A^\beta X_A^\beta \quad (26)$$

Acetic acid material balance

$$\frac{dC_{ac}^\alpha}{dt} = \frac{C_{ac}^\beta - C_{ac}^\alpha}{a\theta/b} + 3.54 \mu_A^\alpha X_A^\alpha + 8.006 \mu_{AP}^\alpha X_{AP}^\alpha + 15.366 \mu_{AB}^\alpha X_{AB}^\alpha - 24.135 \mu_M^\alpha X_M^\alpha \quad (27)$$

$$\frac{dC_{ac}^\beta}{dt} = \frac{C_{ac}^\alpha - C_{ac}^\beta}{(1-a)\theta/b} + 3.54 \mu_A^\beta X_A^\beta + 8.006 \mu_{AP}^\beta X_{AP}^\beta + 15.366 \mu_{AB}^\beta X_{AB}^\beta - 24.13 \mu_M^\beta X_M^\beta \quad (28)$$

Propionic acid material balance

$$\frac{dC_{pc}^\alpha}{dt} = \frac{C_{pc}^\beta - C_{pc}^\alpha}{a\theta/b} + 2.937 \mu_A^\alpha X_A^\alpha - 10.566 \mu_{AP}^\alpha$$

$$\frac{dC_{pc}^\beta}{dt} = \frac{C_{pc}^\alpha - C_{pc}^\beta}{(1-a)\theta/b} + 2.937 \mu_A^\beta X_A^\beta - 10.566 \mu_{AP}^\beta$$

Butyric acid material balance

$$\frac{dC_{but}^\alpha}{dt} = \frac{C_{but}^\beta - C_{but}^\alpha}{a\theta/b} + 3.079 \mu_A^\alpha X_A^\alpha - 11.919 \mu_B^\alpha$$

$$\frac{dC_{but}^\beta}{dt} = \frac{C_{but}^\alpha - C_{but}^\beta}{(1-a)\theta/b} + 3.079 \mu_A^\beta X_A^\beta - 11.919 \mu_B^\beta$$

Ammonia material balance

$$\frac{dC_{am}^\alpha}{dt} = \frac{C_{am}^\beta - C_{am}^\alpha}{a\theta/b} + \frac{17(n-m(1-y_e))}{162+17n} k^\alpha C_{is}^\alpha - 0$$

$$(\mu_A^\alpha X_A^\alpha + \mu_{AP}^\alpha X_{AP}^\alpha + \mu_{AB}^\alpha X_{AB}^\alpha + \mu_M^\alpha X_M^\alpha)$$

$$\frac{dC_{am}^\beta}{dt} = \frac{C_{am}^\alpha - C_{am}^\beta}{(1-a)\theta/b} + \frac{17(n-m(1-y_e))}{162+17n} k^\beta C_{is}^\beta$$

$$0.15(\mu_A^\beta X_A^\beta + \mu_{AP}^\beta X_{AP}^\beta + \mu_{AB}^\beta X_{AB}^\beta + \mu_M^\beta X_M^\beta)$$

Carbon dioxide material balance

$$\frac{dC_c^\alpha}{dt} = \frac{C_c^\beta - C_c^\alpha}{a\theta/b} + 2.413 \mu_A^\alpha X_A^\alpha + 1.01 \mu_{AP}^\alpha X_{AP}^\alpha$$

$$3.303 \mu_{AB}^\alpha X_{AB}^\alpha + 16.726 \mu_M^\alpha X_M^\alpha - \frac{N_c^\alpha}{a V_l}$$

$$\frac{dC_c^\beta}{dt} = \frac{C_c^\alpha - C_c^\beta}{(1-a)\theta/b} + 2.413 \mu_A^\beta X_A^\beta + 1.01 \mu_{AP}^\beta X_{AP}^\beta$$

$$3.303 \mu_{AB}^\beta X_{AB}^\beta + 16.726 \mu_M^\beta X_M^\beta$$

methane material balance

$$\frac{C_m^\beta}{a\theta/b} + 1.509 \mu_{AP}^\alpha X_{AP}^\alpha + 0.956 \mu_{AB}^\alpha X_{AB}^\alpha +$$

$$6.082 \mu_M^\alpha X_M^\alpha - \frac{N_m^\alpha}{a V_l} = 0$$

$$\frac{dC_m^\beta}{dt} = -\frac{C_m^\beta}{(1-a)\theta/b} + 1.509 \mu_{AP}^\beta X_{AP}^\beta +$$

$$0.956 \mu_{AB}^\beta X_{AB}^\beta + 6.082 \mu_M^\beta X_M^\beta$$

Where

$$\theta = \frac{V_l}{Q_f} \quad (39)$$

$$b = \frac{Q_e}{Q_f} \quad (40)$$

### Gas phase

Carbon dioxide material balance

$$\frac{dP_c}{dt} = \frac{R T}{V_g} \left( \frac{N_c^\alpha}{44} - \frac{P_c}{P} F_t \right) \quad (41)$$

Methane material balance

$$\frac{dP_m}{dt} = \frac{R T}{V_g} \left( \frac{N_m^\alpha}{16} - \frac{P_m}{P} F_t \right) \quad (42)$$

Total material balance

$$F_t = \frac{P}{P - P_w} \left( \frac{N_m^\alpha}{16} + \frac{N_c^\alpha}{44} \right) \quad (43)$$

In addition, to apply the pH inhibition effects to the kinetic rate expressions and calculation of the free ammonia and carbon dioxide in the liquid phases, the pH variations with time should be simulated. For this purpose the ionic charge balance equations for the two liquid phases, the dissociation rate equations and the expressions of the total concentration of the ionic components in the liquid phases are developed as a function of the pH. In general, the model is based on the following assumptions and considerations:

1- The uniformity assumptions were considered in the gas phase and the two liquid phases of  $\alpha$  and  $\beta$ .

2- The Monod-type kinetics was applied for the microbial steps (acidogens, acetogens, and methanogens).

3- The non-competitive type inhibition model was considered in all the microbial steps as described in the previous sections.

4- The first order rate was applied to the bacterial decay reaction and the enzymatic hydrolytic steps.

5- The decay rate constants of the different bacterial groups were assumed to be 5% of their maximum growth rate.

6- The mass transfer to the gas phase was only done by the liquid phase of  $\alpha$ .

7- Only the flow-through region was fed with the influent and the effluent streams.

8- The  $\beta$  liquid phase would exchange materials only with the  $\alpha$  liquid phase.

9- The system pressure and reaction volume were considered constant.

10- The energetic effects were not considered and the temperature was perfectly controlled.

11- At the operational temperature and pressure, biogas was considered to be an ideal gas.

12- the biogas consisted of methane,  $\text{CO}_2$  and  $\text{H}_2\text{O}$ .

13- The water vapor in the biogas stream was at saturation state.

14- The  $\text{CO}_2$  present in the  $\alpha$  liquid phase was in thermodynamic equilibrium with the  $\text{CO}_2$  in the gas phase and it obeyed Henry's law as follows:

$$[\text{CO}_2]^\alpha = \frac{C_c^\alpha / 44}{1 + k_{a1} / [\text{H}^+] + k_{a1} k_{a2} / [\text{H}^+]^2} = \frac{1}{F}$$

15- The concentration of methane in the liquid phase was assumed to be negligible, i.e., it was immediately transferred to the gas phase due to its low solubility.

16- In the ionic charge balance (Equation 44), the algebraic sum of the concentrations of the ionic compounds in the process,  $[\text{A}^-\text{C}^+]$ , was assumed constant during the anaerobic digestion process and calculated from the initial pH of the system for the  $\alpha$  and  $\beta$  liquid phases.

$$[\text{H}^+] + [\text{NH}_4^+] = [\text{OH}^-] + [\text{HCO}_3^-] + 2[\text{CO}_3^{2-}] +$$

$$[\text{Ac}^-] + [\text{Pr}^-] + [\text{But}^-] + [\text{A}^-\text{C}^+]$$

17- The times for feeding, draining and mixing were assumed negligible compared to the total batch operation.

The assumptions made in developing the model were mostly based on our previous work [16] and the two-region mixing model was based on Levenspiel [15].

### Computer simulations

The computer simulations were conducted to evaluate the effect of the incomplete mixing on the anaerobic digestion performance of the reactor through the changes on the characteristic parameters  $a$  and  $b$  and also on the operating parameters of the cyclic batch reactor. These simulations were performed by the numeric first order integration of the relevant equations with a fixed time step by

program based on the Euler's method. The program was written in a generalized form in Fortran, where a variable number of steps, feed composition, initial conditions and the operating conditions as well as the kinetic and the mixing parameters of the model could be specified through an input file.

The values of the applied mixing parameters were selected on the basis of the information found in the literature. The tracer studies conducted in the full-scale anaerobic digesters have revealed the well-mixed portions of the digester volumes ranging widely from 23% to 88% [11]. There is less evidence regarding the average interchange rates of the contents in the anaerobic digesters. The kinetic model parameters were taken directly from the literature and are given in Table 1. Also the physio-chemical model parameters at 35 °C are given in Table 2. The manure composition used in the model simulations is given in Table 3 and it was based on the cattle manure used in the experiments of Angelidaki [5].

The ionic charge balance equations should be iteratively solved for the pH calculation since the concentrations of the ionic compounds, in turn, are functions of the pH according to Equations 46 to 52 presented in the following:

The ionic concentrations of different compounds as a function of its total concentration and pH:

$$[\text{NH}_4^+] = \frac{C_{\text{am}}/17}{1 + K_{a6}/[\text{H}^+]}$$

$$[\text{OH}^-] = K_w/[\text{H}^+]$$

$$[\text{HCO}_3^-] = \frac{C_c/44}{1 + [\text{H}^+]/K_{a1} + K_{a2}/[\text{H}^+]}$$

$$[\text{CO}_3^{2-}] = \frac{C_c/44}{1 + [\text{H}^+]/K_{a2} + [\text{H}^+]^2/K_{a1}K_{a2}}$$

$$[\text{Ac}^-] = \frac{C_{\text{ac}}/60}{1 + [\text{H}^+]/K_{a3}}$$

$$[\text{Pr}^-] = \frac{C_{\text{pr}}/74}{1 + [\text{H}^+]/K_{a4}}$$

$$[\text{But}^-] = \frac{C_{\text{but}}/88}{1 + [\text{H}^+]/K_{a5}}$$

Table 1: Kinetic parameters used in the model [6]

Parameter	$K_{ss}$	$K_{spr}$	$K_{sbut}$	$K_{sac}$	$K_{iVFA}$	$K_{ipr}$	$K_{ibut}$	$K_{iam}$	$K$
Unit	g/l	g/l	g/l	g/l	g/l	g/l	g/l	g/l	d
Value	0.5	0.259	0.176	0.12	0.33	0.96	0.72	0.26	1.
Parameter	$\mu_{\text{maxA}}$	$\mu_{\text{maxAP}}$	$\mu_{\text{maxAB}}$	$\mu_{\text{maxM}}$	$y_e$	$n$	$m$	$pK_{hAP}$	$pK$
Unit	d <sup>-1</sup>	d <sup>-1</sup>	d <sup>-1</sup>	d <sup>-1</sup>	---	---	---	---	---
Value	5.0	0.54	0.68	0.6	0.55	0.454	0.34	8.5	6.
Parameter	$pK_{hAB}$	$pK_{IAB}$	$pK_{hM}$	$pK_{IM}$					
Unit	---	---	---	---					
Value	8.5	6.0	8.5	6.0					

Table 2: Physio-chemical parameters at 35 °C [17]

Parameter	$K_w$	$K_{a1}$	$K_{a2}$	$K_{a3}$	$K_{a4}$
Unit	molar	molar	molar	molar	molar
Value	$2.065 \times 10^{-14}$	$4.909 \times 10^{-7}$	$5.623 \times 10^{-11}$	$1.73 \times 10^{-5}$	$1.445 \times 10^{-5}$
Parameter	$K_{a5}$	$K_{a6}$	$H_c$		
Unit	molar	molar	atm.l/mol		
Value	$1.445 \times 10^{-5}$	$1.567 \times 10^{-9}$	37.67 [18]		

Table 3: Characteristics of the feed

Characteristic	Value
Insoluble substrate	30.4 (g/l)
Soluble substrate	5.4 (g/l)
Total acetate	4.5 (g/l)
Total propionate	2.3 (g/l)
Total butyrate	0.2 (g/l)
Total ammonia	3.0357 (gNH <sub>3</sub> /l)
Total carbon dioxide	0.0 (g/l)
Total microbial biomass	0.2 (g/l)
Fraction of acidogens	0.65
Fraction of propionate acetogens	0.025
Fraction of butyrate acetogens	0.025
Fraction of methanogens	0.30
pH	7.0

Of course we need to use an additional iterative procedure for the calculation of the pH of the  $\alpha$  liquid phase, since according to Equation 44, the total concentration of the CO<sub>2</sub> in the  $\alpha$  liquid phase is a function of the pH of this phase and the partial pressure of this gas in the gas phase. A trial-and-error procedure was used to calculate the pH and the different component concentrations of the  $\alpha$  liquid phase.

## RESULTS AND DISCUSSION

The effect of the mixing parameters  $a$  and  $b$  on the distribution of the component concentrations in a cyclic batch reactor with  $t_r = 1$  day and HRT = 12 days are shown in Figures 2 and 3 for the insoluble substrate and propionate, respectively. In these figures the simulation results are compared for the two different sets of the mixing parameters  $a$  and  $b$ , of (0.3,0.5), and (0.3,5.0). As can be seen from Figure 2 for large values of the mixing parameter  $b$ , the value of the insoluble substrate concentration rapidly increases in the retention region and then shows the same pattern of insoluble substrate concentration change in the flow-through region. As the mixing parameter  $b$  is decreased at a constant value of the parameter  $a$ , the pattern of insoluble substrate change in both regions is similar but varies in quantity. In Figure 3, the same variations can be observed for the propionate concentration. As can be seen, the mixing parameter  $b$  has a significant effect on the distribution of components in the reactor so that with increasing this mixing

parameter, the different component concentrations in the  $\alpha$  and  $\beta$  liquid phases become entirely similar. The resulting homogeneous and non-homogeneous medium concentrations throughout the total reactor due to the high and low interchange in tested ranges, shows that the two-region model used to simulate anaerobic reactors with the ideal non-ideal mixing conditions.

The effects of the mixing parameters  $a$  and  $b$  on the methane yield and the CO<sub>2</sub> composition in the biogas are shown in Figures 4 and 5. As can be seen, the methane yield shows high fluctuations as function of the mixing parameters  $a$  and  $b$  equal to 0 respectively. However these variations are less frequent for the other mixing group considered. This observation could be accounted for the complex profile of the different components in the biogas. The methane yield increased with increasing the mixing parameter  $b$  from 0.5 to 5.0 so that the methane production at the steady-state conditions for ( $a = 0.3$  and  $b = 0.5$ ) were equal to 165, and for ( $a = 0.3$  and  $b = 5.0$ ) were equal to 165, and 175 respectively. Also the methane production is lower for the latter mixing parameters group with  $b$  of 0.5 than in the case of the former mixing parameters group. On the other hand, as shown in Figure 5, at the steady-state conditions, the concentration in biogas increases with the mixing. Therefore, it is necessary to apply a mixing condition in the reactor that leads to methane production with lower CO<sub>2</sub> percent which having lower biogas refinery cost.

The steady-state methane yield as a function of the feeding period ( $t_r$ ) is shown in Figure 6 for the cyclic batch reactors with HRTs of 12, 18, and 24 days, respectively. The mixing parameters  $a$  and  $b$  were chosen 0.3 and 0.5, respectively. As can be seen, there is an optimum  $t_r$  corresponding to the maximum methane yield for all three cases. The optimum  $t_r$  value increases with the increase in HRT. For HRTs of 12, 18, and 24 days, the optimum  $t_r$  is 3, 4, and 5 days, respectively. This means that for systems a ratio 3/12, 4/18, and 5/24 of reactor volume should be replaced with entering new raw materials with the reactors. Also, the ratio of  $t_r/(a.HRT)$ , the flow-through region volume that is replaced for these three cases are equal to 0.83, 0.7,



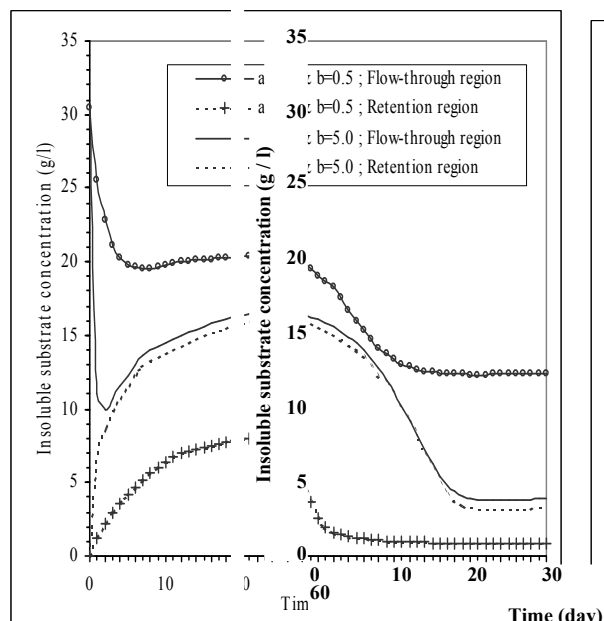


Figure 2. Dynamic simulation of the insoluble substrate concentration in a daily cyclic batch reactor with HRT=12 days and the different degrees of mixing for the prediction of the insoluble substrate concentration.

Fig. 2: Dynamic simulation of the insoluble substrate concentration in a daily cyclic batch reactor with HRT=12 days and the different degrees of mixing for the prediction of the insoluble substrate concentration.

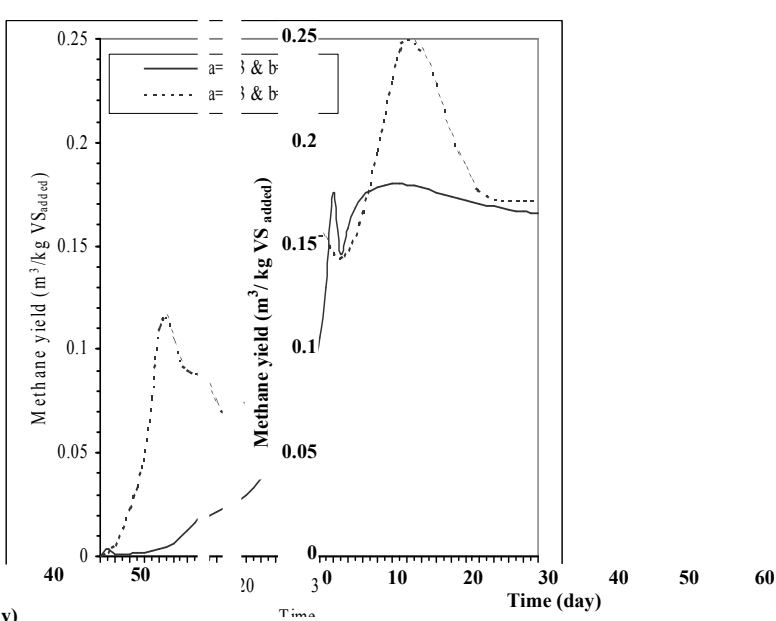


Figure 4. Dynamic simulation of the methane yield in a daily cyclic batch reactor with HRT=12 days and the different degrees of mixing for the prediction of the methane yield.

Fig. 4: Dynamic simulation of the methane yield in a daily cyclic batch reactor with HRT=12 days and the different degrees of mixing for the prediction of the methane yield.

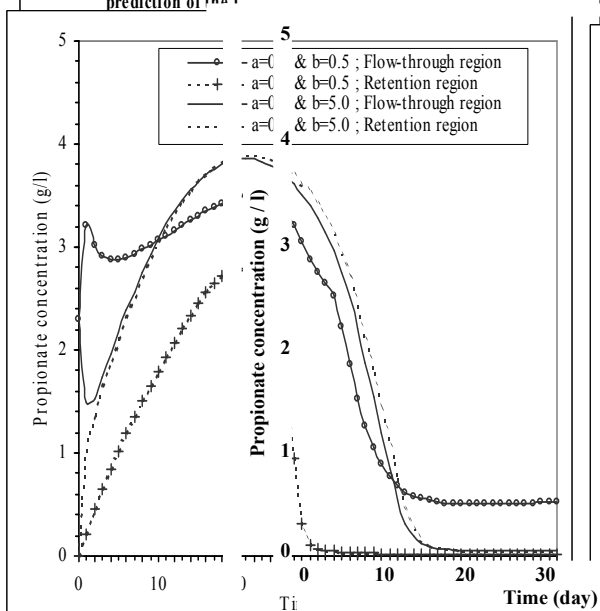


Figure 3. Dynamic simulation of the propionate concentration in a daily cyclic batch reactor with HRT=12 days and the different degrees of mixing for the prediction of the propionate concentration.

Fig. 3: Dynamic simulation of the propionate concentration in a daily cyclic batch reactor with HRT=12 days and the different degrees of mixing for the prediction of the propionate concentration.

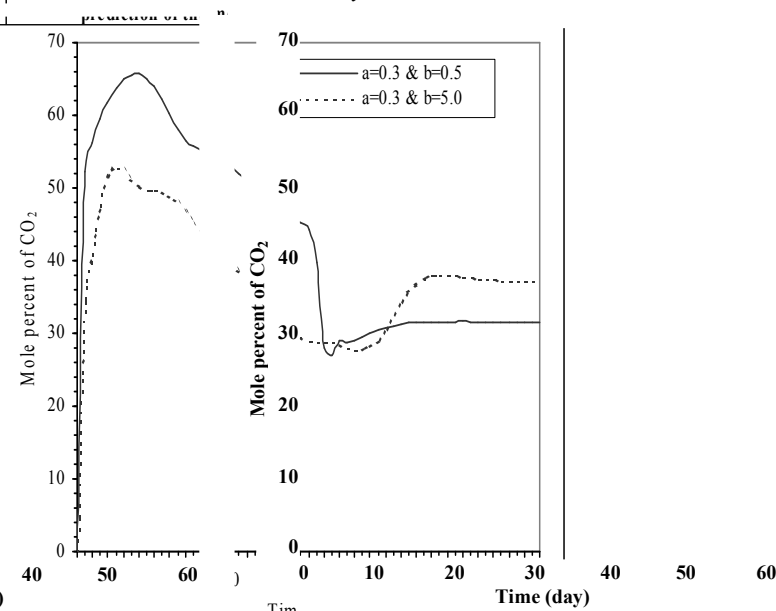


Figure 5. Dynamic simulation of the CO2 mole percent in biogas in a daily cyclic batch reactor with HRT=12 days and the different degrees of mixing for the prediction of the CO2 mole percent in biogas.

Fig. 5: Dynamic simulation of the CO2 mole percent in biogas in a daily cyclic batch reactor with HRT=12 days and the different degrees of mixing for the prediction of the CO2 mole percent in biogas.

respectively. It is seen that the methane yield at the optimum conditions for the system with the ratio of  $t_r/(a.HRT)$  equal to 0.69 is higher than two other systems. Therefore, it can be concluded that there is an optimum ratio of  $t_r/(a.HRT)$  for cyclic-batch reactors in the range of 0.6-0.8 that gives the maximum methane yield.

The effect of the hydraulic retention time on the methane yield was evaluated for two different reactors including a daily-fed non-ideally mixed cyclic batch reactor ( $a=0.3$  and  $b=0.5$ ,  $t_r=1$  day) and an approximately non-ideally mixed continuous flow reactor ( $a=0.3$  and  $b=0.5$ ,  $t_r=0.1$  day). The steady-state results are shown in Figure 7. As is seen, there is an HRT critical range for both reactors. For an HRT smaller than this critical range due to the cell wash-out, the accumulation of the VFAs and a sharp decline in the pH, the anaerobic digestion process becomes unstable and a sour reactor is created. This results in a sharp decrease in the methane production. In contrast, for the HRT values greater than the critical range, the change in methane yield vs HRT depends on the type of feeding which may increase or decrease with a slow slope. The unexpected decrease of the methane yield with increase in HRT in the case of cyclic-batch regime can be explained by the change in the ratio  $t_r/(a.HRT)$ . This value decreases from 0.22 to 0.06 by increasing HRT from 15 to 50 days. Therefore, the methane yield decreases as the value of  $t_r/(a.HRT)$  goes beyond its optimum range. As can be seen from Figure 7, the performance of the continuous flow reactor in terms of methane production is better than the cyclic batch reactor.

The effect of mixing parameter  $a$ , on the steady-state methane yield at conditions that the mixing parameter  $b$  is equal to 0.5 is illustrated in Figure 8 for the three different systems. In the first system, a cyclic-batch reactor with a  $t_r$  of 2 days and an HRT of 24 days, and in the second and third systems, an approximately continuous flow reactor ( $t_r = 0.1$ ) with an HRT of 24 and 12 days, have been simulated. As expected theoretically, in the continuous flow regime, the methane yield increases with the increase in the mixing parameter  $a$  (corresponding to a decreased dead zone volume in the reactor). Also, it is seen that the effect of mixing parameter  $a$  on the degree of variations of the methane yield in continuous flow reactors decreases with the increase in HRT from 12 to 24 days because the organic

materials find further time for mixing and discharge the reactor. Therefore, the effect of the degree on the methane yield becomes less important. An unexpected decrease in the methane yield increase in the mixing parameter  $a$  for a cyclic batch reactor can be explained, as mentioned earlier, by the change in the value of  $t_r/(a.HRT)$ . When the mixing parameter  $a$  increases from 0.3 to 0.6, the ratio  $t_r/(a.HRT)$  decreases from 0.28 to 0.14 being an optimum value of 0.69.

The effect of mixing parameter  $b$  on the methane yield at conditions that the mixing parameter  $a$  is equal to 0.3 is illustrated in Figure 9 for three different systems. In the first system, a cyclic batch reactor with a  $t_r$  of 2 days and an HRT of 1 day, and in the second and third systems, an approximately continuous flow reactor ( $t_r = 0.1$ ) with an HRT of 12 and 24 days have been simulated. As is seen, the methane yield increases with the increase in the mixing parameter  $b$  in all cases. In continuous flow reactor, it is observed that the effect of mixing parameter  $b$  on the increase in the methane yield reduces with an increase in the HRT from 12 to 24 days. In other words, the degree of mixing becomes less important with increased retention time of the materials in the reactor.

To evaluate the applicability of the model, preliminary simulations were compared to experimental runs [19] measuring methane production at various organic loading rates for an HRT of 6 days to determine the most appropriate set of mixing parameters. The operating conditions of their experiments are given in Table 4. In Figure 10, the best fit of the experimental data is shown. The estimated HRT/ $b$  mixing parameters of the reactor are 0.3 and 4.0, respectively. Steady-state methane yield at an HRT of 6 days were then predicted for different organic loading rates using the mixing parameters. Predicted values are compared with experimental values in Figure 11. As can be seen, a good agreement between the predicted values and the experimental values is observed.

## CONCLUSIONS

The performance of anaerobic digestion is dependent on the degree of mixing achieved in the reactor. However, it is difficult and expensive

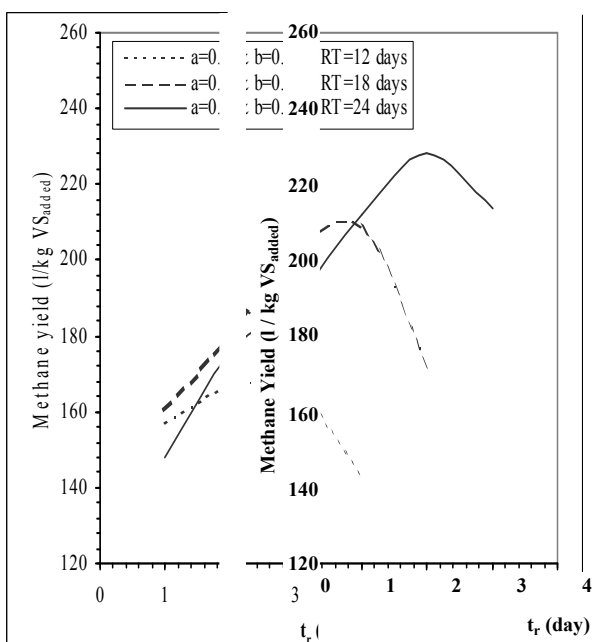


Figure 6. Effect of the time period of feeding on the steady-state methane yield at different HRTs.

Fig. 6: Effect of the time period of feeding on the steady-state methane yield at different HRTs.

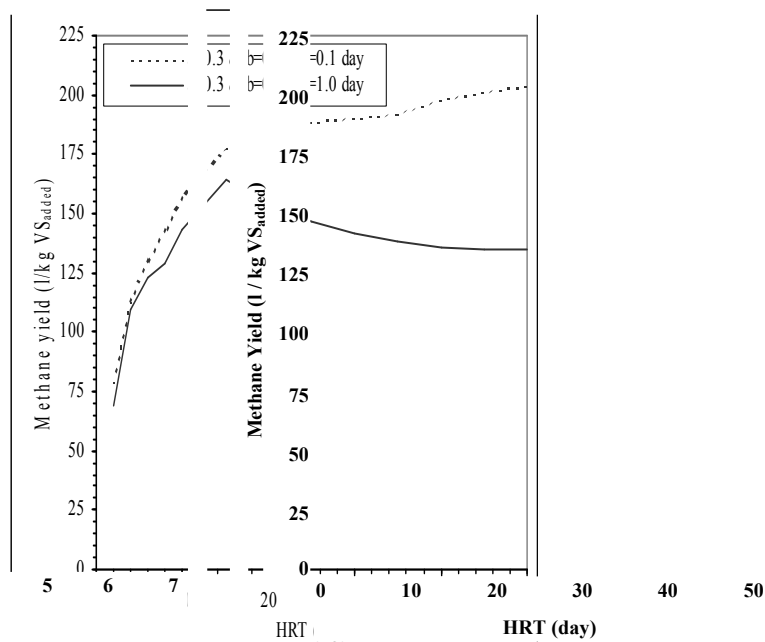


Figure 7. Effect of the hydraulic retention time on the steady-state methane yield.

Fig. 7: Effect of the hydraulic retention time on the steady-state methane yield.

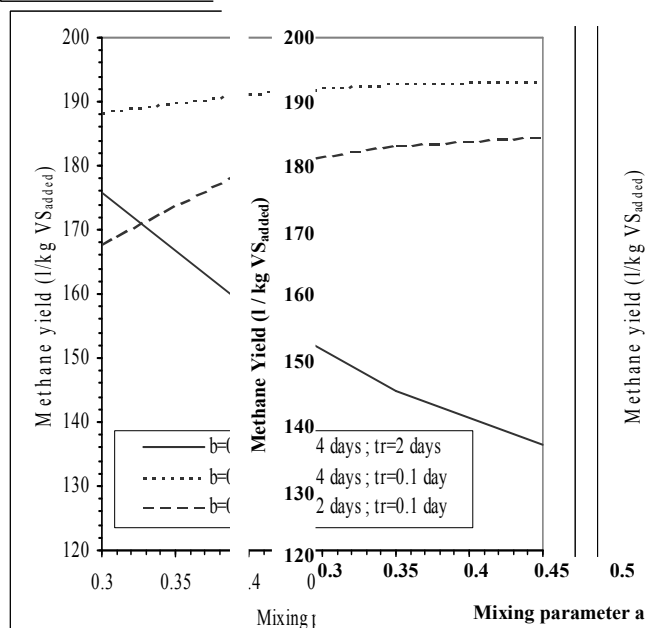


Figure 8. Effect of the relative volume region (a) on the steady-state methane yield at different HRTs.

Fig. 8: Effect of the relative volume region (a) on the steady-state methane yield at different HRTs.

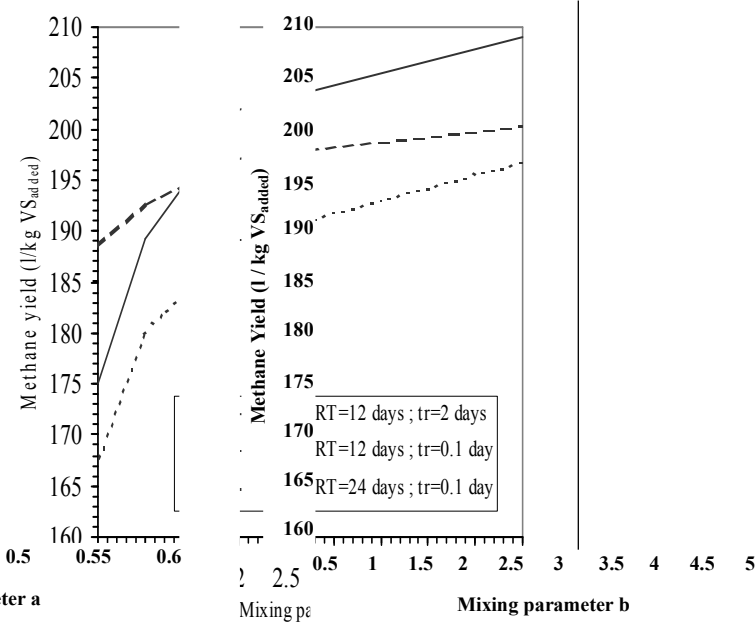


Figure 9. Effect of the internal exchange flow rate to the feed flow rate ratio (b) on the steady-state methane yield at different HRTs.

Fig. 9: Effect of the internal exchange flow rate to the feed flow rate ratio (b) on the steady-state methane yield at different HRTs.

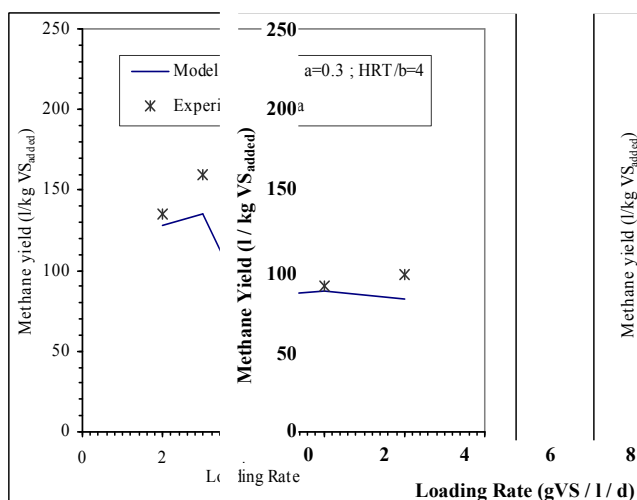


Figure 10. Model data (Dugba and yield-organic load appropriate set of

Fig. 10: Model prediction versus experimental methane yield – organic loading rate for appropriate set of mixing parameters.

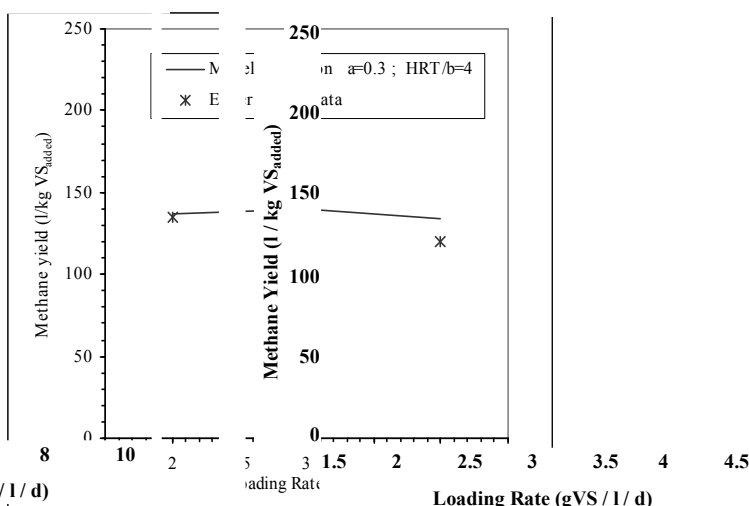


Figure 11. Comparison between experimental data [19] and the prediction of methane yield as a function of the organic loading rate.

Table 4: Operating parameters of the reactor

Operational parameters	Values
Total volume	15 liters
Temperature	35 °C
pH	Controlled at 6.7-7.3
Mixing of reactor	1 minute every hour
VS loading rate for HRT=3 days	2,3,4,6,8 gVS/l/day
VS loading rate for HRT=6 days	2,3,4 gVS/l/day

a complete mixing in full scale reactors. Therefore, the real reactors are often operated under non-ideal mixing conditions. The performance of the anaerobic digestion processes can be predicted by an appropriate mathematical model. Unfortunately, in most available models, the simplified assumptions of the complete mixing conditions are used, and consequently their applicability appears to be limited. The simulation results showed that the two-region mixing model, despite its simplicity, can be used for modeling of the non-ideally mixed reactors with different degrees of mixing. Analysis of the impact of the characteristic mixing parameters on the anaerobic digestion of the cattle manure showed that the reactor performance is a complex

function of both mixing parameters. With mixing as depicted by the two-region model, the degree of mixing affects the residence time distribution of components in the reactor. Consequently, the kinetic rates of the anaerobic digestion are influenced. Also it is observed that the degree of feeding as well as the mixing parameter distribution of components in the reactor. It is observed that there is an optimum ratio of  $t_r/(a.HRT)$  for reactors resulting in the maximum methane production. The simulation results shows that the reactor performance is improved when the period of feeding approaches the continuous flow regime. The obtained results emphasize the importance of mixing consideration when simulating the anaerobic digestion process and consequently in designing the reactor. The two-region mixing model can be used for the simulation of the anaerobic digestion whose mixing patterns resemble such a mixing pattern. The characteristic mixing parameters of the two-region mixing model can be calculated from the experimental tracer-response curves and by fitting the experimental data to the model by using the least-square method.

#### Acknowledgment

The authors would like to express their appreciation to the



:Comment

for the financial support provided by Center of Renewable Energies for Research and Application and Dr. M. Khalagi Asadi, the head of the center.

### Nomenclature

a	mixing parameter
b	mixing parameter
C	liquid concentration (g/l)
[CO <sub>2</sub> ]	free CO <sub>2</sub> in liquid concentration (mol/l)
d	day
f <sub>pr</sub>	mass conversion factor of propionate to acetate=0.8108
f <sub>but</sub>	mass conversion factor of butyrate to acetate=0.6818
F <sub>t</sub>	biogas transfer rate (mol/d)
F(pH)	pH function
H	Henry's constant (atm.l/mol)
HRT	hydraulic retention time
K	hydrolysis rate constant (d <sup>-1</sup> )
K <sub>0</sub>	non-inhibited hydrolysis rate constant (d <sup>-1</sup> )
K <sub>a1</sub>	first dissociation constant of carbonic acid
K <sub>a2</sub>	second dissociation constant of carbonic acid
K <sub>a3</sub>	dissociation constant of acetic acid
K <sub>a4</sub>	dissociation constant of propionic acid
K <sub>a5</sub>	dissociation constant of butyric acid
K <sub>w</sub>	dissociation constant of water
K <sub>d</sub>	bacterial decay rate constant (d <sup>-1</sup> )
K <sub>i</sub>	inhibition constant (g/l)
K <sub>s</sub>	Monod saturation constant (g/l)
m	feed constant used in Equation 1
n	feed constant used in Equation 1
N	gas transfer rate (g/d)
[NH <sub>3</sub> ]	free NH <sub>3</sub> in liquid concentration (mol/l)
P	pressure (atm)
pK <sub>h</sub>	constant used in Equation 16
pK <sub>1</sub>	constant used in Equation 16
Q	volumetric flow rate (l/d)
r <sub>d</sub>	bacterial decay rate (g/l.d)
r <sub>h</sub>	hydrolysis reaction rate (g/l.d)
r <sub>s</sub>	substrate consumption rate (g/l.d)
r <sub>x</sub>	bacterial growth rate (g/l.d)
R	gas constant (atm.l/mol.K)
R	recycle flow ratio defined in Equation 18

t	time (d)
T	temperature (°K)
V <sub>g</sub>	gas volume of reactor (l)
V <sub>l</sub>	liquid volume of reactor (l)
VFA	volatile fatty acids
X	microorganisms concentration
y <sub>e</sub>	yield factor used in Equation 10
Y <sub>s/x</sub>	yield factor of biomass
A	flow-through region
β	retention region
θ	hydraulic retention time (d)
μ	specific growth rate (d <sup>-1</sup> )
μ <sub>max</sub>	maximum specific growth rate

### Subscripts

ac	acetate
am	ammonia
A	acidogenic bacteria
AB	butyric degrading acetogenic
AP	propionate degrading acetogenic
but	butyrate
c	carbon dioxide
e	exchange between zones
f	feed
i	component i
i	initial conditions
is	insoluble substrate
m	methane
M	methanogenic bacteria
pr	propionate
r	effluent flow
s	soluble substrate
w	water

Received: 21<sup>st</sup> October 2001 ; Accepted: 25<sup>th</sup>

### REFERENCES

- [1] Constant, M., Naveau, H., Ferrero, J. L. a J., Biogas end-uses in the European C Elsevier Science Publishing Company, (1989).
- [2] Andrews, J. F., Dynamic model of the digestion process., *J. Sanit. Engng Div. Soc. Civ. Engrs SA* 1, 95-116, (1969).

- [3] Buhr, H. O. and Andrews, J. F., The thermophilic anaerobic digestion process., *Water Res.*, **11**, 129-143, (1977).
- [4] Hill, D. T. and Barth, C. L., A dynamic model for simulation of animal waste digestion., *J. Water Pollut. Control Fed.*, **49**, 2129-2143, (1977).
- [5] Angelidaki, I. and Ahring, B. K., Thermophilic anaerobic digestion of livestock waste: The effect of ammonia., *Appl. Microbiol. Biotechnol.*, **38**, 560-564, (1993).
- [6] Angelidaki, I., Ellegaard L. and Ahring, B. K., A mathematical model for dynamic simulation of anaerobic digestion of complex substrates: Focusing on ammonia inhibition., *Biotech. and Bioengng.*, **42**, 159-166, (1993).
- [7] Buffiere, P., Steyer, J. P., Fonade, C. and Moletta, R., Comprehensive modeling of methanogenic biofilms in fluidized bed systems: Mass transfer limitations and multisubstrate aspects., *Biotech. and Bioengng.*, **48**, 725-736, (1995).
- [8] Kalyuzhnyi, S.V. and Davlyatshina, M.A., Batch anaerobic digestion of glucose and its mathematical modeling., *Bioresource Technology*, **59**, 73-80, (1997).
- [9] Batstone, D.J., Keller, J., Newell, R. B. and Newland, M., Modeling anaerobic degradation of complex wastewater., *Bioresource Technology*, **75**(1), 67-74, (2000).
- [10] Nielsen, J. and Villadsen, J., Modeling of microbial kinetics., *Chem. Engng Sci.*, **47**, 4225-4270, (1992).
- [11] Montieth, H. D. and Stephenson, J. P., Mixing efficiencies in full-scale anaerobic digesters by tracer methods., *J. WPCF*, **53**, 78-84, (1981).
- [12] Kalia, A.K. and Knawar, S. S., Long-term of a fixed dome Janata biogas plant conditions., *Bioresource Technology*, (1998).
- [13] Ong, H.K., Greenfield, P.F. and Pullamr P. C., An operational strategy for biomethanation of cattle manure slurry in a unmixed single stage digester., *Bioresource Technology*, **73**(1), 87-89, (2000).
- [14] Sterling, M. C., Jr., Lacey, R. E., Engle, Ricke, S. C., Effect of ammonia nitrogen on  $CH_4$  production during anaerobic digestion of cattle manure., *Bioresource Technology*, **18**, (2001).
- [15] Levenspiel, O., "Chemical Reaction Engineering", Second Edition, Wiley & Sons Book New York, (1972).
- [16] Keshtkar, A., Ghaforian, H., Abolhan Meyssami, B., Dynamic simulation of continuous anaerobic digestion of cattle manure., *Bioresource Technology*, **80**, 9-17, (2001).
- [17] Dean, J. A., "Lange's Handbook of Chemistry", Fourteenth Edition, McGraw Hill Book New York, (1992).
- [18] Archer, D. B., *Enzyme Microbiol. Technol.*, **167**, (1983).
- [19] Dugba, P. N., Zhang, R., Treatment of wastewater with two-stage anaerobic sequencing batch reactor systems- thermophilic versus mesophilic operations., *Bioresource Technology*, **6**, (1999).